Low-Viscosity Triethylbutylammonium Acetate as a Task-Specific Ionic Liquid for Reversible CO_2 Absorption

Guannan Wang, Wenlong Hou, Feng Xiao, Jiao Geng, Youting Wu,* and Zhibing Zhang*

Separation Engineering Research Center, School of Chemistry and Chemical Engineering, Nanjing University, Nanjing, 210093, P. R. China

S *Supporting Information*

ABSTRACT: Capturing and storing carbon dioxide (CO_2) is now of concern. This work presents a task-specific ionic liquid (TSIL), triethylbutylammonium acetate ($[N_{2224}][CH_3COO]$), for the purpose of trapping CO_2 instead of the commonly used organic amine solutions. Since $[N_{2224}][CH_3COO]$ has a hydrophilic nature, the CO_2 dissolution behavior into $[N_{2224}][CH_3COO]-nH_2O$ complexes has been investigated in detail, including the absorption rate, absorption capacity, and the ability of repeating absorption. The solubilities of CO_2 into $[N_{2224}][CH_3COO]-1H_2O$ at 0 °C, 25 °C, 40 °C, and 60 °C from (0.007 up to 30) bar are presented. The results show strong evidence that $[N_{2224}][CH_3COO]-1H_2O$ is an excellent reversible absorbent for CO_2, and the recovered $[N_{2224}][CH_3COO]-1H_2O$ maintains the same absorption capacity and absorption rate. The CO_2 absorption into $[N_{2224}][CH_3COO]-nH_2O$ mixtures at 25 °C and pressures up to 30 bar is also studied. It is elucidated that the absorption capacity decreases with the content of water and the rise of operational temperature. The equilibrium constant, Henry's law constant, overall rate constant, and activation energy are also calculated from the experimental data. All evidence indicates that $[N_{2224}][CH_3COO]-nH_2O$ with low viscosity may have potential to be used as good absorbents for CO_2 capture.

INTRODUCTION

The increasing concentration of atmospheric CO_2 is becoming a prominent global environmental issue today. Under the cap of the European Union ETS (Emission Trading Scheme), major European countries have to face the pressure of CO_2 emission reduction in appointed sectors, e.g., iron and steel, power generation, refining, etc. China, as a developing country, also suffers seriously from such problems. Therefore, how to trap and store CO_2 efficiently and safely, especially when the concentration of CO_2 is relatively small in the atmosphere (0.03 %) and in the industrial flue gases (volume fraction is from 10 % to 15 %[1]), is a huge challenge for science researchers and chemical engineers.

Nowadays, technologies of trapping CO_2 using inorganic base solutions,[2] limestones,[3] and aqueous organic amines[4] as absorbents are extensively carried out in chemical plants. However, these technologies are often accompanied with resource consumption due to the irreversible reaction of absorbents with CO_2 (in the case of inorganic base solutions and limestones) or organic pollutants releasing to the atmosphere and aqua-sphere[5] (in the case of aqueous organic amines). Additionally, high operation costs and large consumption of energy are also drawbacks of these processes.[2,6] As an alternative to traditional organic solvents, ionic liquids (ILs) provoke a wide interest in the scientific community and in industrial fields, involving its applications in organic synthesis,[7,8] catalysis,[9,10] supercritical fluid reaction,[11] and gas separation[12] due to their outstanding characteristics such as negligible vapor pressure,[13] high thermal stability,[14] and so on.[15,16] Comparing to the volatile amines as sequestering agents, ILs possess the nonvolatile and thermal stable characteristics that make them environmentally benign gas absorbents[17] without causing concurrent loss of the liquid into the gas and then polluting the environment.

Some pioneering works have shown that ILs could reversibly trap acidic gases, e.g., CO_2 and SO_2,[18-21] and extensive efforts were followed on studying the improvement of CO_2 solubility in ILs.[18,19] It is found that some CO_2-philic functional groups, such as fluorine,[20] carbonyl groups,[18] and dicyanamide,[11] are good for CO_2 capture. However, due to the potential contaminations and high cost,[21] many researches have paid much attention to the functionalization of ILs by designing the structures of both cations and anions according to the practical needs and special purposes, so that task-specific ionic liquids (TSILs) for absorbing CO_2 with high capacity and high selectivity could be obtained.[26-28] Others tried to utilize the ILs in facilitated transport membranes or on porous silica gel for acidic gas separations.[29-31] To our knowledge, most supported membrane processes have to be applied under the constraints of their small industrial scales, whereas most TSILs such as amine-appended ILs confront the unexpected high viscosity that causes long absorption equilibrium time and unfavors the mass and heat transfers during the absorption. Therefore, reducing the viscosity of TSILs is becoming a critical issue for practical applications.

Tetraethylammonium α-alanine ($[N_{2222}][L\text{-}Ala]$) with a low viscosity (81 mPa·s, at 25 °C) has been reported in our previous work,[22] and it showed good potential to act as a CO_2 trapper. It was indicated that the small amino acid anion plays a key role in reducing the viscosity of $[N_{2222}][L\text{-}Ala]$. Quinn et al.[23] claimed that melts of salt hydrates such as tetraethylammonium acetate

tetrahydrate ($[(C_2H_5)_4N][CH_3COO]\cdot 4H_2O$) exhibited large CO_2 absorption capacities. Yokozeki[34,35] and Compton[24] both demonstrated that ionic liquids with acetate anions show very high solubility of CO_2. Inspired by these achievements, it may be a promising way to create tailor-made molten salts with an asymmetric quaternary ammonium cation and a weak carboxylate anion to diminish the viscosity and maintain the absorption capacity.

This paper describes, for the first time, a task-specific ionic liquid $[N_{2224}][CH_3COO]$ and its water complexes for the capture of CO_2. In this work, NMR, EA, IR, and Karl Fischer analysis were used to determine the structure, the presence of the water, and the purity. A test device was designed to determine the solubility of CO_2 into the samples. On the basis of the absorption experimental data, the chemical equilibrium constant, Henry's law constant, overall rate constant, and activation energy are also calculated.

■ EXPERIMENTAL SECTION

Materials. Butyl bromide (AR grade, $\geq$ 99.0 %) and silver acetate (AgAc) (AR grade) were purchased from Sinopharm Chemical Reagent Co., Ltd. (Nanjing, China). Triethylamine (AR grade) and ethanol with a purity of $\geq$ 99.5 % were obtained from Nanjing Chemical Reagent Co., Ltd. (Nanjing, China). Carbon dioxide was from Nanjing Weichuang Gas Co., Ltd. (China) with a minimum purity of 99.99 %.

Preparation and Characterization of $[N_{2224}][CH_3COO]-$ nH_2O. The preparation of $[N_{2224}][CH_3COO]$ followed a two-step procedure. Butyltriethylammonium bromide ($[N_{2224}][Br]$) was prepared by reacting triethylamine with bromobutane in ethanol under refluxing conditions for 48 h. After removing the solvent, white solid was dried at 60 °C overnight under vacuum. The objective product $[N_{2224}][CH_3COO]$ was obtained from the equimolar metathesis reaction of $[N_{2224}][Br]$ with AgAc in the mixed solvent of ethanol and water (volume fraction was 50 %) for 24 h. After centrifugation and filtration, a gray green precipitate was removed. The filtrate was dried at 90 °C for five days, leading to a light yellow paste of $[N_{2224}][CH_3COO]$ with a yield of 84 % (based on the moles of triethylammonium). If the filtrate was dried at 70 °C for two days, it led to a light yellow liquid of $[N_{2224}][CH_3COO]-1H_2O$ with a yield of 82.4 %. The concentration of the bromine ion in $[N_{2224}][CH_3COO]$ was measured by Mohr titration, and the related impurity was less than 0.02 %. The final sample had a calculated Ag^+ concentration of parts per billion level from the limited solubility product of AgBr. The viscosity and density were measured by a cone–plate viscometer (HAAKE Rheostress 600, an uncertainty of $\pm$ 1 % in relation to the full scale) and a densitometer (Anton Paar, DMA 5000 DENSITYMETER, an uncertainty of $\pm$ 0.03 kg·m^{-3}), respectively. The water in the compounds was determined by ^{1}H NMR (BRUKER DPX 300), EA (Elementar vario EL II), FTIR (BRUKER Vector 22), and Karl Fischer Analysis (Metrohm, 787KF Titrino). The decomposition temperature, melting temperature, water loss temperature, and glass transition temperature were determined from the TG (PerkinElmer, Pyris 1 TGA) and DSC (PerkinElmer, DTA7) from (−100 to 400) °C. The DSC instrument was calibrated by the standard reference indium and zincum sample, and the uncertainty was $\pm$ 0.2 °C. Since the calorimetric accuracy was 1 %, with respect to the glass transition temperatures and melting temperatures, overall uncertainty for the DSC and TG determinations was estimated to be $\pm$ 2 K. The $[N_{2224}][CH_3COO]-2H_2O$ was prepared by adding 2 mol of water into 1 mol of $[N_{2224}][CH_3COO]$, while $[N_{2224}]$

$[CH_3COO]-5H_2O$ was obtained by adding 5 mol of water into 1 mol of $[N_{2224}][CH_3COO]$.

Determination of CO_2 Absorption. The absorption reactor is made of stainless steel, and it can afford pressures up to 120 bar. The whole test device consists of an isothermal water bath, absorption equilibrium, and data receiving sections. This device has two chambers, and the bigger chamber (90.14 cm^3) isolates CO_2 before it contacts with the samples in the smaller chamber (33.13 cm^3) that is equipped with a magnetic stirrer. The temperature of both chambers is controlled by the water bath to be $\pm$ 0.1 K. The CO_2 pressures in the two chambers are monitored using two pressure gauges (WIDEPLUS PRECISION INSTRUMENTS CO., LTD) of $\pm$ 0.2 % uncertainty (in relation to the full scale). A known mass (w) of sample [(3 to 5) g] was placed into the smaller chamber with the magnetic stirrer for the measurement of CO_2 solubility. A vacuum (< 10 Pa) was then drawn to degas the whole device for at least 2 h. While the two chambers were separated using a needle valve, the bigger chamber received known amounts of CO_2, measured by one pressure gauge (p_1). The needle valve between the two chambers was turned on to let CO_2 be introduced to the sample in the smaller chamber. Absorption equilibration was thought to be obtained when the pressures (p_1' and p_2) of the two chambers remained constant for at least 1 h. After reaching equilibration, the CO_2 uptake, $n(p_2)$, can be calculated using the following equation

$$n(p_2) = \rho_g(p_1, T)V_1 - \rho_g(p_1', T)V_1 - \rho_g(p_2, T)(V_2 - w/\rho_{IL})$$

(1a)

where $\rho_g(p_i, T)$ is the density of CO_2 in mol·cm^{-3} at p_i ($i = 1, 2$) and T, and ρ_{IL} is the density of the ionic liquid sample in g·cm^{-3} at T. V_1 and V_2 represent the volumes in cm^3 of the two chambers, respectively. Continual determinations of solubility data at elevated pressures were performed by introducing more CO_2 into the smaller chamber to reach new equilibrations, and the calculation equation should be modified as

$$n(p_2) = \rho_g(p_1, T)V_1 + [\rho_g(p_0, T)(V_2 - w/\rho_{IL}) + n(p_0)]$$
$$- \rho_g(p_1', T)V_1 - \rho_g(p_2, T)(V_2 - w/\rho_{IL}) \quad (1b)$$

where p_0 stands for the equilibrium pressure of the last solubility value determined. The term in the square bracket on the right side accounts for the CO_2 mass resident already in the smaller chamber. Duplicate experiments for each sample were run to obtain averaged solubility values and their uncertainties. To test the accuracy of the absorption apparatus, the solubility of CO_2 into 1 M NaOH solution and $[bmim][PF_6]$ was determined and compared with those in the references (see Supporting Information). The results in Tables S4 to S5 and Figures S11 to S12 demonstrated the uncertainty of the absorption measurement using the apparatus in this work to be within $\pm$ 0.1 %.

■ RESULTS AND DISCUSSION

Chemical Structure and Physical Parameters. The ^{1}H NMR and FT-IR characterization results of the samples are shown in Figure 1. Results of other characterizations such as ^{13}C NMR, EA, TG, and DSC can be seen in the Supporting Information. All peaks in ^{1}H NMR and FT-IR spectra are in a good agreement with the corresponding chemical structure. Comparing the results of ^{1}H NMR (300 MHz, DMSO, 25 °C,
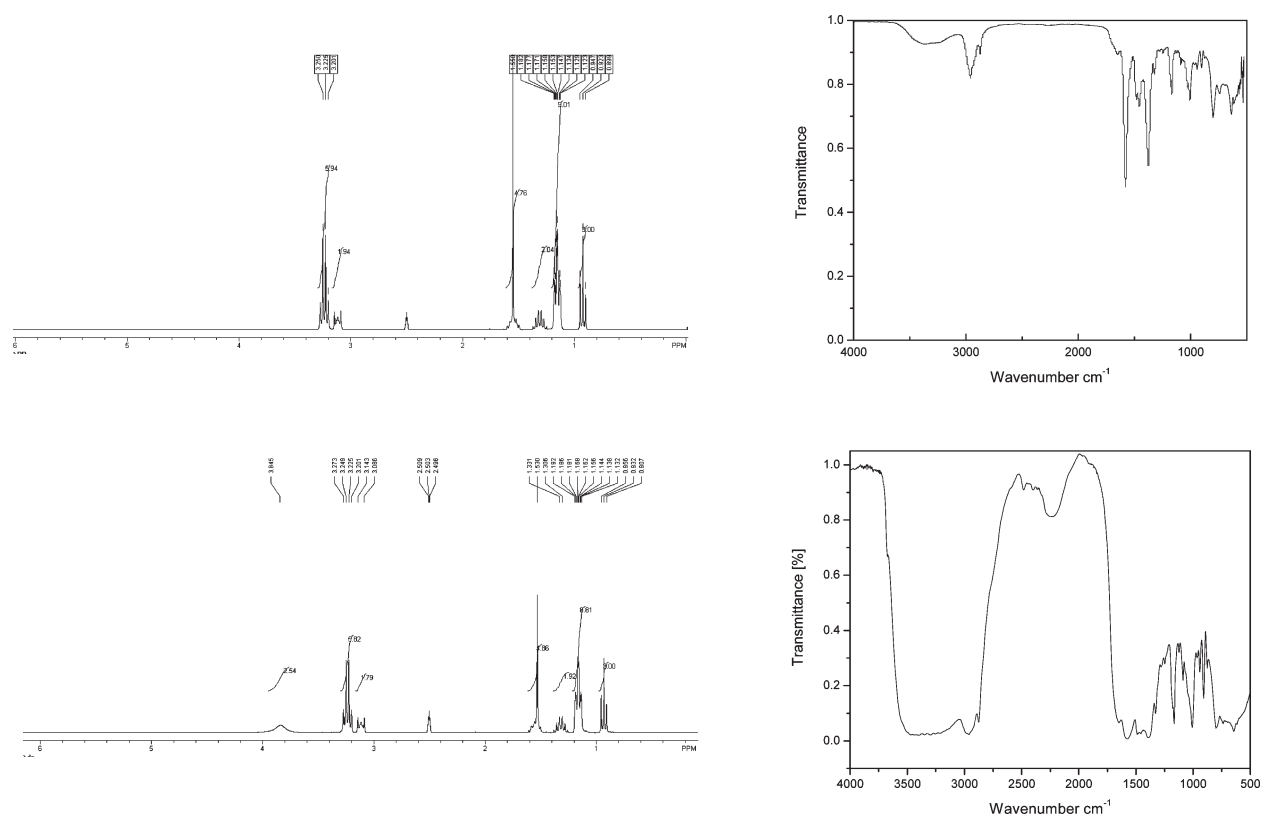
Figure 1. ^{1}H NMR and FTIR spectra of $[N_{2224}][CH_3COO]$ (upper) and $[N_{2224}][CH_3COO]-1H_2O$ (lower).

Table 1. Physical Parameters of $[N_{2224}][CH_3COO]$ and $[N_{2224}][CH_3COO]-1H_2O^a$

complex	T_g °C	T_f^a °C	ΔC_p J·g^{-1}·°C^{-1}	T_m °C	T_{dec} °C	T_{water} °C	ρ/g·cm^{-3} (25 °C)	η/mPa·s (25 °C)	water content g·g^{-1}
$[N_{2224}][CH_3COO]$	ND	16.1	ND	27.7	171	ND	0.9883	439	<0.001
$[N_{2224}][CH_3COO]-1H_2O$	−72.3	ND	0.809	ND	175	103	0.9837	79	0.089

^{a} ND, not detected; T_f^a, temperature that IL freezes; T_{water}, temperature that complex loses its water.

TMS) between $[N_{2224}][CH_3COO]$ and $[N_{2224}][CH_3COO]-1H_2O$, the only difference is the appearance of water. The chemical shift of the corresponding ^1H_2O in $[N_{2224}][CH_3COO]-1H_2O$ is 3.845 ppm, and the integrated areas of the resonance at 3.845 ppm refer to two H atoms. This implies the mole ratio between H_2O and $[N_{2224}][CH_3COO]$ is 1:1, agreeing well with the water content determined from Karl Fischer Analysis which is 0.089 g·g^{-1}.

Table 1 lists some crucial physical parameters such as glass transition temperature (T_g), melting temperature (T_m), decomposition temperature (T_{dec}), ΔC_p value, water content, density (ρ), and viscosity (η) of $[N_{2224}][CH_3COO]$ and $[N_{2224}][CH_3COO]-1H_2O$. The DSC curve shows a distinct melting temperature of $[N_{2224}][CH_3COO]$ at 27.7 °C, which strongly supports that the sample is a room-temperature ionic liquid. Furthermore, the sample starts to freeze at 16.1 °C, suggesting that $[N_{2224}][CH_3COO]$ is in a stable supercooled state. The viscosity of $[N_{2224}][CH_3COO]$ is 439 mPa·s at 25 °C. The higher viscosity of $[N_{2224}][CH_3COO]$ than [bmim][CH$_3$CO-O] (140 mPa·s)[25] may be the result of larger molecular weight of the tetraalkylammonium cation, and the viscosity of functionalized

Table 2. Viscosities in mPa·s of $[N_{2224}][CH_3COO]$ and Its Water Complexes at Different Temperatures

complex	298.2 K	313.2 K	333.2 K
$[N_{2224}][CH_3COO]$	439	306.7	47.3
$[N_{2224}][CH_3COO]-1H_2O$	79	55.5	15.6
$[N_{2224}][CH_3COO]-2H_2O$	66	39.4	12.6
$[N_{2224}][CH_3COO]-5H_2O$	13	10.9	5.15

ionic liquid obtained in this work is far smaller than those of the dual amino functional phosphomium ILs[26] (lowest value is 713.9 mPa·s). Interestingly, the viscosity of $[N_{2224}][CH_3COO]$ can be reduced dramatically to 79 mPa·s with the addition of 1 mol of H_2O. It is obvious that the presence of water in ILs, as well as the increase of temperature, can reduce the viscosity. The viscosities of $[N_{2224}][CH_3COO]$ and its water complexes are determined at different temperatures and summarized in Table 2. The viscosity of $[N_{2224}][CH_3COO]$ decreases to 47.3 mPa·s at 60 °C, and viscosities of its water complexes are all lower than 80 mPa·s at all three experimental temperatures. It is also clearly shown in Table 1 that $[N_{2224}][CH_3COO]-1H_2O$ is a liquid in a wide

1127

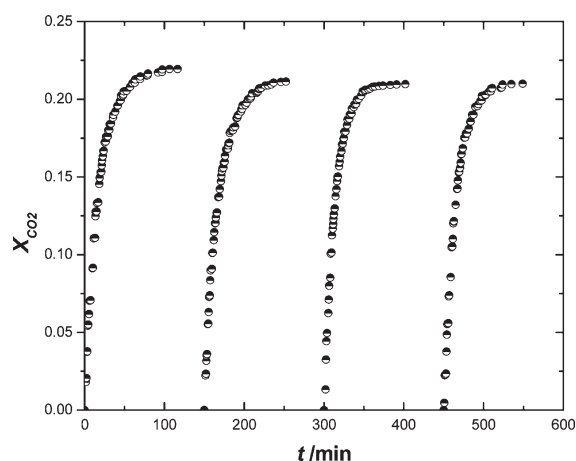dx.doi.org/10.1021/je101014q |*J. Chem. Eng. Data* 2011, 56, 1125–1133

Figure 2. Reversible absorption of CO_2 into $[N_{2224}][CH_3COO]-1H_2O$ at 298.2 K and the same initial pressure of 1 bar.

range of temperatures from (-50 to 100) °C in contrast to $[N_{2222}][CH_3COO]-4H_2O$ (T_m = 45 °C).[27] This diversity proves that an asymmetric cation can reduce the melting temperature of the ionic liquid. In addition, only a glass transition temperature is shown at -72.3 °C, and the decomposition temperature is 175 °C. An extra thermal stability test of $[N_{2224}][CH_3COO]-1H_2O$ using isothermal DSC at 100 °C for 24 h (see Supporting Information) shows that the complex loses approximately a quarter of its mass (including the mass of water) in 24 h and suffers from the lack of thermal durability. $[N_{2224}][CH_3COO]-1H_2O$ has a lower glass transition temperature than that of the asymmetric tetraalkylphosphonium amino acid ionic liquids (ranging from (-69.7 to -29.6) °C),[26] indicating a large window of liquid state that favors industrial purpose. In particular, it was found that the viscosity of $[N_{2224}][CH_3COO]-1H_2O$ (79 mPa·s, 25 °C) is a little lower than that of $[N_{2222}][L\text{-Ala}]$ (81 mPa·s, 25 °C),[22] which may be primarily attributed to the asymmetry of the cation. The cation with an asymmetric structure is more flexible and has larger free volume than the symmetric one because the butyl chain is longer than the ethyl. Furthermore, the weak alkaline anion has the nature of hydrophilic, and water diminishes the viscosity.[28] This may be another reason for the lower viscosity of $[N_{2224}][CH_3COO]-1H_2O$ than that of $[N_{2222}][L\text{-Ala}]$. Both samples in this work have a little lower densities than $[bmim][CH_3COO]$ (1.053 g·cm^{-3} at 298.2 K),[29] implying a larger molar liquid volume.

Absorption of CO_2. Repeated absorption of CO_2 into $[N_{2224}][CH_3COO]-1H_2O$ at the same initial pressure of 1 bar was investigated, and the results were shown in Figure 2. The absorption isotherms reach 95 % of the equilibrium value in less than 45 min. After finishing the absorption, the complex was recovered by removing CO_2 in a vacuum oven ($\approx$1 kPa) at 70 °C for 4 h so that the ability of reversible absorption could be examined. The absorption experiments were repeated four times. Because an absolute vacuum was not actually achieved, the incomplete desorption of CO_2 during the recovery of the used IL resulted in the absorption capacity in the first cycle being about 4 % greater than those in the other three cycles. The results in Figure 2 demonstrated that $[N_{2224}][CH_3COO]-1H_2O$ can absorb CO_2 reversibly and efficiently.

Figure 3 shows the CO_2 solubility in $[N_{2224}][CH_3COO]-1H_2O$ at 0 °C, 25 °C, 40 °C, and 60 °C and pressures from (0 up to 30) bar. The isotherms are plotted as the mole fraction of CO_2

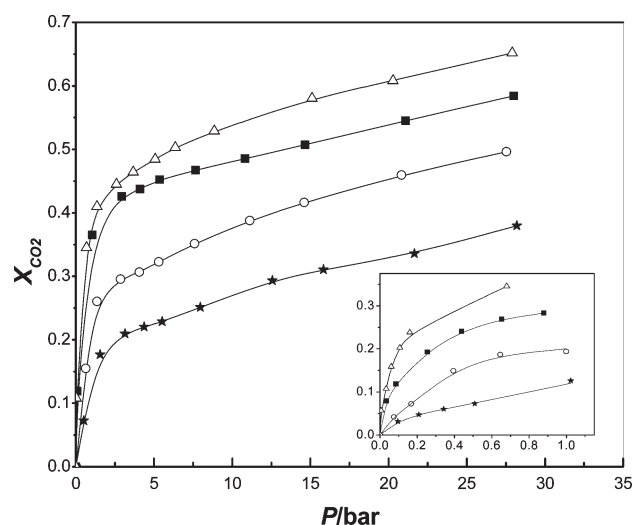**Figure 3.** CO_2 solubility into $[N_{2224}][CH_3COO]-1H_2O$ at various temperatures and pressures of CO_2. Symbols △, ■, ○, and ★ represents the experimental data at 273.2 K, 298.2 K, 313.2 K, and 333.2 K, respectively.
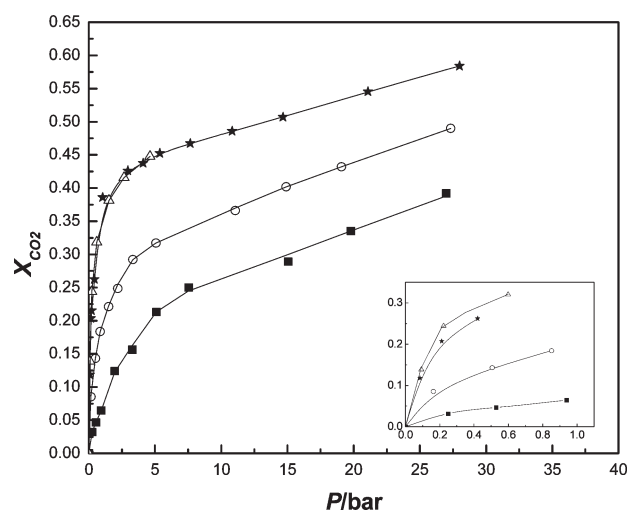

Figure 4. Influence of water content on the absorption capacity of $[N_{2224}]$ $[CH_3COO]-nH_2O$ at 298.2 K. △, ★, ○, and ■ represents the experimental data of $[N_{2224}][CH_3COO]$, $[N_{2224}][CH_3COO]-1H_2O$, $[N_{2224}]$ $[CH_3COO]-2H_2O$, and $[N_{2224}][CH_3COO]-5H_2O$, respectively.

(X_{CO2}) in the liquid phase versus the equilibrium pressure of CO_2. The inset plots in Figure 3 are the behavior of CO_2 dissolution at pressures lower than 1 bar. The isotherms are found to rise up dramatically fast when the pressure is lower than 3 bar and then tend to increase linearly and slowly with the increasing pressure. The gradient of the isotherm with a steep rise at lower pressure, together with the evidence of bicarbonate and acetic acid formation (see the analysis in the next section), indicates that the $[N_{2224}][CH_3COO]-1H_2O$ mixture has a large chemical affinity for CO_2.[23] Then, the isotherms clearly show a linear dependence on absorption capacity on pressures from (3 to 30) bar, inferring that the mixtures absorb CO_2 mainly via a physical absorption mechanism in this pressure range. In addition, the CO_2 solubility decreases with the increasing temperature, which is in accordance with the demonstrated results found in most cases of gas dissolution into liquid.
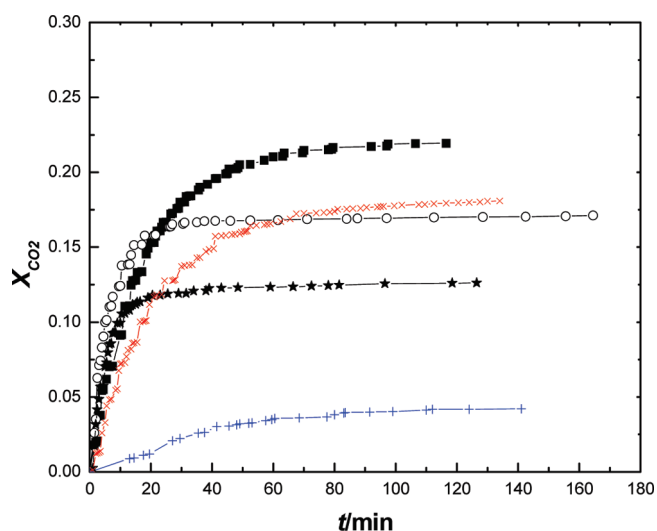
Figure 5. Absorption capacities and equilibrium times for complexes with different water at different temperatures and the same initial pressure of 1 bar. Lines with ■, ○, and ★ symbols represent the experimental data of $[N_{2224}][CH_3COO]-1H_2O$ at 298.2 K, 313.2 K, and 333.2 K, respectively, and the line with × and + symbols represents the experimental data of $[N_{2224}][CH_3COO]-2H_2O$ and $[N_{2224}][CH_3COO]-5H_2O$ at 298.2 K, respectively.

The CO_2 solubility into $[N_{2224}][CH_3COO]-nH_2O$ complexes at 25 °C with respect to pressure is present in Figure 4, showing that the excess amount of water is a negative factor for the absorption of CO_2. The inset plots in Figure 4 are the behavior of CO_2 dissolution at pressures lower than 1 bar. $[N_{2224}][CH_3COO]$ has a little larger absorption capacity than its water complexes, and this fact can be explained using different reaction mechanisms. Without water, $[N_{2224}][CH_3COO]$ can only absorb CO_2 via a Lewis acid and base reaction,[29] while the $[N_{2224}][CH_3COO]-nH_2O$ are via another mechanism which will be discussed in the next section. However, $[N_{2224}][CH_3COO]$ becomes a thick paste after 5 bar and restrains further experiments at higher CO_2 partial pressures, whereas $[N_{2224}][CH_3COO]-nH_2O$ are still flowable throughout the whole experimental CO_2 pressure range.

Lines with "■", "×", and "+" symbols in Figure 5 represent, respectively, the time-dependent dissolution processes of CO_2 into $[N_{2224}][CH_3COO]-1H_2O$, $[N_{2224}][CH_3COO]-2H_2O$, and $[N_{2224}][CH_3COO]-5H_2O$ at 25 °C and at the same initial pressure of 1 bar. The isotherms of the $2H_2O$ and $5H_2O$ complexes are lower than that of the $1H_2O$ sample, suggesting also that the absorption capacity is negatively influenced by the increasing amount of water. This is in accordance with the results in Figure 4. The three isotherms in Figure 5 with a solid square, hollow circle, and solid asterisk symbols represent the absorption capacity and absorption rate of $[N_{2224}][CH_3COO]-1H_2O$ at 25 °C, 40 °C, and 60 °C and the same initial pressure of 1 bar, respectively. At 60 °C and 40 °C, the absorption equilibria are reached within 15 min and 25 min, respectively. Comparing among these three isotherms, it can be concluded that high temperature promotes the rate of the absorption but reduces CO_2 affinity. This demonstrates that the absorption rate is a strong function of temperature. When the temperature increases, the molecules in the liquid phase are activated, and the viscosity of the sample is reduced, so that the mass transfer rate increases.

Mechanism of CO_2 Dissolution in $[N_{2224}][CH_3COO]-nH_2O$ Complexes. Assuming that the water molecules are connected with the acetate anions by a hydrogen bond in the $[N_{2224}][CH_3COO]-nH_2O$ complexes, eq 2 was claimed by Quinn et al.,[23] and it was proved to be suitable for our case from the results of ^1H NMR, ^{13}C NMR, and FT-IR (see Supporting Information) before and after $[N_{2224}][CH_3COO]-nH_2O$ were saturated with CO_2. The newly appeared peaks in the FT-IR spectrum for the CO_2 adduction are 1396, 1458, and 1488 cm^{-1}. These peaks represent the vibration of the O—H in the H_2O molecule. Additionally, there is an extra resonance signal at 2.084 ppm in the CO_2-saturated IL detected by ^1H NMR spectra as well as a new signal at 31.008 ppm in ^{13}C NMR spectra. Combining this chemical reaction mechanism with the analytical results stated above, it is apparent that the bicarbonate and acetic acid are formed during the exposure of $[N_{2224}][CH_3COO]-nH_2O$ to the CO_2 environment. If the acetate anion loses its basicity, the chemical reaction reaches the equilibrium. From then on, the complexes capture CO_2 in a physical manner, mainly by hydrogen bonding or van der Waals force. When the $[N_{2224}][CH_3COO]-nH_2O$ ($n > 1$) react with CO_2, the affinity between the acetate anion and CO_2 is reduced because the acetate anion combines more water molecules instead. Additionally, the reaction product acetic acid is also accompanied with water. It is commonly understood that the acetic acid with a small amount of water is more stable than pure acetic acid. In other words, reactions involving $[N_{2224}][CH_3COO]-nH_2O$ ($n > 1$) complexes easily reach the CO_2 saturation because of the formation of a stable acetic acid—H_2O compound.

$$CH_3COO^- - nH_2O + CO_2 \rightleftharpoons HCO_3^-$$
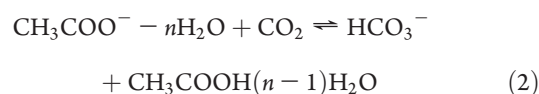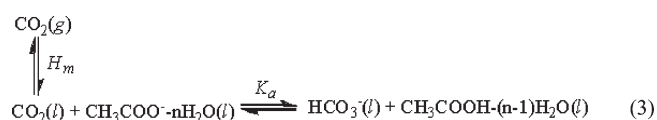$$+ CH_3COOH(n-1)H_2O \qquad (2)$$

Table 3 lists different uptakes of CO_2 into several ILs, together with their viscosities and times required for reaching absorption equilibrium. Obviously, an IL with lower viscosity spends less time to reach the absorption equilibrium. The viscosity is essentially determined by the volume, molecular weight, and structure of ions. On the basis of our former experience about the preparation of amino acid ionic liquid with low viscosity, the small molecular weight of ions and a flexible alkyl chain can reduce the viscosity.[22] Besides, a small volume[30] and asymmetric structure[31] of the ions can also lead to the decrease of viscosity, and the presence of water or organic solvents[32] is an external contribution for low viscosity. The reason for the viscosity of $[N_{2224}][CH_3COO]-1H_2O$ being lower than that of $[N_{2222}][L-Ala]$ has already been discussed. It is widely accepted that the nature of anions has the most significant influence on the solubility of CO_2, whereas the cations give less contribution.[20] Comparing the CO_2 solubility of $[N_{2222}][L-Ala]$ with that of $[N_{2224}][CH_3COO]-1H_2O$, it is demonstrated clearly that the acetate anion has more power of enhancing the CO_2 solubility than the α-alanine anion. The differences in the absorption behavior between $[N_{2224}][CH_3COO]-1H_2O$ and $[N_{2222}][CH_3COO]\cdot1H_2O$[37] should be attributed to the cations. The butyl chain in the $[N_{2224}]$ makes the cation asymmetric and more flexible than $[N_{2222}]$, so that $[N_{2224}][CH_3COO]-1H_2O$ is imaginable to be of larger free volume, the reason being easier CO_2 mass uptake in $[N_{2224}]$-based compounds. For the same reason, the larger CO_2 capacity of $[N_{2224}][CH_3COO]-1H_2O$ than that of $[emim][CH_3COO]$ and $[bmim][CH_3COO]$ can also be imputable to the cation since the long alkyl chains in

1129

dx.doi.org/10.1021/je101014q |*J. Chem. Eng. Data* 2011, 56, 1125–1133

Table 3. Comparison of Absorption Properties of Various ILs at 25 °C and 1 bar

compounds	CO_2 mole fraction	mass ratio of CO_2 to IL	time for reaching absorption equilibrium	molecular weight	$\eta/\text{mPa} \cdot \text{s}$
			min	$\text{g} \cdot \text{mol}^{-1}$	(25 °C)
$[N_{2222}][\text{L-Ala}]^{22}$	0.325	0.0970	60	218.31	81
$[\text{emim}][CH_3COO]^{34}$	0.267	0.0942		170.21	162
$[\text{bmim}][CH_3COO]^{34}$	0.275	0.0842	60	198.26	140
$[N_{2222}][CH_3COO] \cdot H_2O^{27}$	0.319	0.0994		207.32	/
$[N_{2224}][CH_3COO]-H_2O$	0.386	0.1175	45	235.37	79
$[N_{2224}][CH_3COO]-2H_2O$	0.197	0.0426	40	253.39	66
$[N_{2224}][CH_3COO]-5H_2O$	0.054	0.0082	25	307.45	13

$[N_{2224}]$ expand the space between the species that allows for the extensive loading of CO_2.

Henry's Law Constant and Chemical Equilibrium Constant. The solubility of CO_2 into $[N_{2224}][CH_3COO]-nH_2O$ is quite different from the common ILs such as $[\text{bmim}][PF_6]$ because both chemical and physical absorptions occur simultaneously. The solubility behavior of CO_2 has to be described using not only Henry's law constant (H_m) but also the reaction equilibrium constant (K_a). Therefore, eq 2 can be rewritten as

$$CO_2(g)$$
$$\Big\updownarrow H_m$$
$$CO_2(l) + CH_3COO^- \cdot nH_2O(l) \underset{}{\overset{K_a}{\rightleftharpoons}} HCO_3^-(l) + CH_3COOH \cdot (n\text{-}1)H_2O(l) \qquad (3)$$

where the subscript "m" in H_m represents the molality scale, and g and l represents the gas and liquid states of the reactants, respectively. The Henry's law constant is defined as

$$H_m(T, p) \equiv \lim_{m \longrightarrow 0} \frac{f^g}{m} \approx \lim_{m \longrightarrow 0} \frac{p}{m} \qquad (4)$$

where $H_m(T, p)$ is Henry's law constant; $m/\text{mol} \cdot \text{kg}^{-1}$ is the molality of CO_2 dissolved in the liquid phase; f^g is the fugacity of CO_2; and p is the equilibrium pressure. From eq 4, the CO_2 solubility is linearly related to the CO_2 fugacity in the limit of low solute concentrations, and Henry's law constant can be obtained by calculating the slope of the isotherm in this limit. However, the true solubility of CO_2 is different from the theoretical value calculated from eq 4 because the chemical reaction happens.

The chemical reaction equilibrium constant for the reaction in eq 3 can be defined as

$$K_a = \frac{\alpha_3 \cdot \alpha_4}{\alpha_1 \cdot \alpha_2} = \frac{m_3 \cdot m_4}{m_1 \cdot m_2} \cdot \frac{\gamma_3 \cdot \gamma_4}{\gamma_1 \cdot \gamma_2} = K_m \cdot K_\gamma \qquad (5)$$

where α_1, α_2, α_3, and α_4 represent the activities of CO_2, $CH_3COO^- - nH_2O$, HCO_3^-, and $CH_3COOH-(n-1)H_2O$ species in eq 3, respectively; m_1, m_2, m_3, and m_4 represent the concentrations; and γ_1, γ_2, γ_3, and γ_4 are the activity coefficients of these species. Since the complex–CO_2 mixture of low CO_2 concentration obeys Henry's law,[4] it can be considered as an ideal diluted solution, so that $\gamma_3\gamma_4/\gamma_1\gamma_2 = 1$.[33] Thus, we have

$$K_a \cong K_m = \frac{m_3 \cdot m_4}{m_1 \cdot m_2} \qquad (6)$$

where

$$m_3 = m_4 \qquad (7)$$

The gas–liquid equilibrium follows Henry's law because the ideal diluted solution is assumed

$$p = H_m \cdot m_1 \qquad (8)$$

Combining eqs 6, 7, and 8 leads to eq 9

$$m_3 = \left[\frac{p \cdot K_m \cdot m_2}{H_m} \right]^{1/2} \qquad (9)$$

The total concentration of CO_2 in the liquid phase, $M/\text{mol} \cdot \text{kg}^{-1}$, is the summation of free CO_2 and HCO_3^-

$$M = \frac{p}{H_m} + \left[\frac{p \cdot K_m \cdot m_2}{H_m} \right]^{1/2} \qquad (10)$$

Rewriting eq 10, we have

$$\frac{M}{p} = \left[\frac{K_m \cdot m_2}{H_m} \right]^{1/2} \cdot p^{-1/2} + \frac{1}{H_m} \qquad (11)$$

Equation 11 implies that M/p is linearly related to $p^{-1/2}$. After plotting M/p versus $p^{-1/2}$, the values of K_m and H_m can be calculated from the intercept and the slope of the straight line. The experimental data in the range from 0 to 1 bar are adopted for the calculation of H_m and K_m, and since the solubility of CO_2 under 1 bar is relatively small, the concentration of the complex (m_2 in eq 11) can also be approximately treated as a constant under such a circumstance. The values of H_m and K_m for $[N_{2224}][CH_3COO]-1H_2O$ in the temperature range of (273.2 to 333.2) K are obtained and shown in Table 4. Henry's law constants of the $[N_{2224}][CH_3COO]-nH_2O$ system are much smaller than those of imidazolium ionic liquids with $[BF_4]$, $[PF_6]$, or $[Tf_2N]$ anions.[19,35,36] The magnitude of Henry's law constants can classify whether the absorption is the physical or chemical type. Usually, a small value of Henry's law constants less than 3 MPa at 298 K would be the case of chemical absorption for CO_2 into ILs.[34] The chemical equilibrium constant is related to the standard enthalpy change of the chemical reaction via eq 12

$$\ln \frac{K_m}{K_m^{\Theta}} = -\frac{\Delta H_r}{R} \left(\frac{1}{T} - \frac{1}{T_0^{\Theta}} \right) \qquad (12)$$

Equation 12 indicates that $\ln K$ is in a linear relationship with $1/T$. The standard enthalpy change of the chemical reaction can be calculated from the slope of the line. The value of ΔH_r is found to be only $-29 \text{ kJ} \cdot \text{mol}^{-1}$, being relatively small but larger than the enthalpy change induced by hydrogen-bond interactions.

Table 4. Chemical Equilibrium Constant, Henry's Law Constant, and Overall Rate Constant For $[N_{2224}][CH_3COO]-nH_2O-CO_2$ Systems at Different Temperatures

	T			H_m	k	
complex	K	K_m	σ of K_m	$bar \cdot kg \cdot mol^{-1}$	min^{-1}	σ of k
$[N_{2224}][CH_3COO]-1H_2O$	273.2	10.9 ± 0.04	0.997	5.14 ± 0.13	$0.0482 \pm 1.9 \cdot 10^{-4}$	0.999
$[N_{2224}][CH_3COO]-1H_2O$	298.2	3.70 ± 0.011	0.989	13.5 ± 0.14	$0.145 \pm 2 \cdot 10^{-4}$	0.998
$[N_{2224}][CH_3COO]-1H_2O$	313.2	1.99 ± 0.01	0.999	19.0 ± 0.13	$0.195 \pm 1.1 \cdot 10^{-3}$	0.999
$[N_{2224}][CH_3COO]-1H_2O$	333.2	1.04 ± 0.014	0.992	22.9 ± 0.15	$0.251 \pm 1.3 \cdot 10^{-3}$	0.998
$[N_{2224}][CH_3COO]-2H_2O$	298.2	2.78 ± 0.01	0.999	17.1 ± 0.13	$0.0472 \pm 2.3 \cdot 10^{-4}$	0.997
$[N_{2224}][CH_3COO]-5H_2O$	298.2	0.463 ± 0.009	0.999	28.9 ± 0.13	$0.036 \pm 1.6 \cdot 10^{-4}$	0.998

The small enthalpy change implies the good reversibility of the reaction between CO_2 and $[N_{2224}][CH_3COO]-1H_2O$. In addition, Henry's law constants of CO_2 are obtained and correlated using the following equation with an average deviation of 3 %

$$\ln(H_m/bar \cdot kg \cdot mol^{-1}) = 66.43 - 0.093(T/K) \\ - 10753.4/(T/K) \quad (13)$$

The thermodynamic properties of CO_2 dissolution into $[N_{2224}][CH_3COO]-1H_2O$ can also be calculated from the correlation of Henry's law constant based on the following relationships

$$\Delta_{sol}G = RT \ln(H_m(T,p)/p^{\Theta}) \quad (14)$$

$$\Delta_{sol}H = R\left(\frac{\partial \ln(H_m(T,p)/p^{\Theta})}{\partial(1/T)}\right)_p \quad (15)$$

$$\Delta_{sol}S = (\Delta_{sol}H - \Delta_{sol}G)/T \quad (16)$$

$$\Delta_{sol}C_p = \left(\frac{\partial \Delta_{sol}H}{\partial T}\right)_p \quad (17)$$

At the standard temperature and pressure (T^{Θ} = 298.15 K, P^{Θ} = 0.1 MPa), the values (on the molality scale) of $\Delta_{sol}G$, $\Delta_{sol}H$, $\Delta_{sol}S$, and $\Delta_{sol}C_p$ are found to be 6.45 $kJ \cdot mol^{-1}$, -20.67 $kJ \cdot mol^{-1}$, $-90.96 \, J \cdot mol^{-1} \cdot K^{-1}$, and $461.06 \, J \cdot mol^{-1} \cdot K^{-1}$, respectively. From these data, it is obvious that besides taking part in the chemical reaction with CO_2 $[N_{2224}][CH_3COO]-1H_2O$ can absorb CO_2 physically in a similar way with those common ILs such as $[bmim][PF_6]$[37] due to the similarity in these thermodynamic properties.

Reaction Rate and Activation Energy. Equation 2 is a second-order reaction, and the CO_2 absorption rate of the reaction can be expressed as

$$r = k' \cdot C_{IL} \cdot C_{CO2} \quad (18)$$

It is reasonable to assume that only a small part of $[N_{2224}][CH_3COO]-nH_2O$ complexes has been chemically reacted with CO_2 before reaching 10 % of its equilibrium absorption. The concentration of the absorbent is nearly constant compared to the pressure variation during this period, so that eq 18 becomes a first-order reaction for CO_2 and the absorption rate equation can be rewritten as

$$r = -dC_{CO2}/dt = k \cdot C_{CO2} \quad (19)$$

where k is the overall rate constant of the absorption reaction.

Integrating eq 19[38] generates eq 20

$$\ln\frac{p - p^*}{p_0 - p^*} = kt \quad (20)$$

where p is the pressure of CO_2 at time t; p^* is the saturated pressure of CO_2 after the absorption equilibrium is reached; and p_0 is the initial pressure of CO_2 at the beginning of the absorption. From eq 20, the overall reaction rate constant k can be acquired from the plot of $\ln(p - p^*)/(p^0 - p^*)$ versus t.

Table 4 presents the values of k for $[N_{2224}][CH_3COO]-nH_2O$ complexes at various conditions. The temperature dependence of the chemical reaction rate constant can be described using the Arrhenius equation

$$\ln k = -\frac{E_a}{RT} + A \quad (21)$$

where A is a constant. Correlating the reaction rate constants with $1/T$ in the temperature range from (273.2 to 333.2) K according to eq 21 leads to the activation energy for the chemical reaction. The activity energy is found to have a value of 21.1 $kJ \cdot mol^{-1}$ with a correlation coefficient (σ) of 0.974. This value of energy barrier is much smaller than that of methyldiethanolamine (MDEA) reacting with CO_2 (44.3 $kJ \cdot mol^{-1}$),[39] implying the higher reactivity of CO_2 with $[N_{2224}][CH_3COO]-nH_2O$ complexes.

■ CONCLUSIONS

Task-specific ionic liquid $[N_{2224}][CH_3COO]$ and its water complexes of low cost are readily prepared. The physicochemical properties as well as the solubility of CO_2 in the synthesized compounds are reported. The extremely high CO_2 absorption capacity in $[N_{2224}][CH_3COO]-nH_2O$ mixtures makes this compound more attractive than other CO_2 absorbents in industry processes. This performance is due to the choice of the $[N_{2224}]$ cation and the acetate anion because of its large free volume and the basicity. Unfortunately, the thermal stability of the water complexes needs to be improved in future work. Anyway, this work provides a general thought of designing a task-specific ionic liquid for efficient and fast CO_2 capture. In addition, adequate theoretical knowledge of the CO_2 dissolution behavior is necessary in case of getting optimal operation conditions for utilizing the absorbents in industrial processes. In this respect, the reaction equilibrium constant, Henry's law constant, the overall rate constant, and activation energy have been calculated from the experimental data. The halogen-free character, strong CO_2 affinity, and low cost make the $[N_{2224}][CH_3COO]$ and its water complexes more prospective to be applied in CO_2 scrubbing processes. However, further examination

is required to understand how the water molecules affect the absorption capacity in the complexes.

■ ASSOCIATED CONTENT

ⓢ Supporting Information. Tables S1 to S5, Figures S1 to S13, and data for Figures 2 to 5. This material is available free of charge via the Internet at http://pubs.acs.org.

■ AUTHOR INFORMATION

Corresponding Author
*E-mail: ytwu@nju.edu.cn; zbzhang@nju.edu.cn. Phone: +86-25-83593772. Fax: +86-25-83593772.

■ ACKNOWLEDGMENT

■ REFERENCES

(1) Rao, A. B.; Rubin, E. S. A technical, economic, and environmental assessment of amine-based CO_2 capture technology for power plant greenhouse gas control. *Environ. Sci. Technol.* **2002**, *36* (20), 4467–4475.

(2) Cullinane, J. T.; Rochelle, G. T. Thermodynamics of aqueous potassium carbonate, piperazine, and carbon dioxide. *Fluid Phase Equilib.* **2005**, *227* (2), 197–213.

(3) Ryu, H. J.; Grace, J. R.; Lim, C. J. Simultaneous CO_2/SO_2 capture characteristics of three limestones in a fluidized-bed reactor. *Energy Fuels* **2006**, *20* (4), 1621–1628.

(4) Kundu, M.; Bandyopadhyay, S. S. Solubility of CO_2 in water plus diethanolamine plus N-methyldiethanolamine. *Fluid Phase Equilib.* **2006**, *248* (2), 158–167.

(5) Chinn, D.; Vu, D. Q.; Driver, M. S.; Boudreau, L. C. CO_2 removal gas using ionic liquid absorbents. U.S. Patent US7,527,775,B2, May 5, 2009.

(6) Park, S. H.; Lee, K. B.; Hyun, J. C.; Kim, S. H. Correlation and prediction of the solubility of carbon dioxide in aqueous alkanolamine and mixed alkanolamine solutions. *Ind. Eng. Chem. Res.* **2002**, *41* (6), 1658–1665.

(7) Polshettiwar, V.; Varma, R. S. Microwave-assisted organic synthesis and transformations using benign reaction media. *Acc. Chem. Res.* **2008**, *41* (5), 629–639.

(8) Bogel-Łukasika, E.; Santosa, S.; Rafał, B.-Ł.; Nunes, d. P. M., Selectivity enhancement in the catalytic heterogeneous hydrogenation of limonene in supercritical carbon dioxide by an ionic liquid. *J. Supercrit. Fluids* **2010**.

(9) Choi, D. S.; Kim, J. H.; Shin, U. S.; Deshmukh, R. R.; Song, C. E. Thermodynamically- and kinetically-controlled Friedel-Crafts alkenylation of arenes with alkynes using an acidic fluoroantimonate(V) ionic liquid as catalyst. *Chem. Commun.* **2007**, No. 33, 3482–3484.

(10) Li, H. L.; Yu, S. T.; Liu, F. S.; Me, C. X.; Li, L. Synthesis of dioctyl phthalate using acid functionalized ionic liquid as catalyst. *Catal. Commun.* **2007**, *8* (11), 1759–1762.

(11) Bogel-Lukasik, R.; Najdanovic-Visak, V.; Barreiros, S.; da Ponte, M. N. Distribution ratios of lipase-catalyzed reaction products in ionic liquid supercritical CO_2 systems: Resolution of 2-octanol enantiomers. *Ind. Eng. Chem. Res.* **2008**, *47* (13), 4473–4480.

(12) Brennecke, J. F.; Maginn, E. J. Ionic liquids: Innovative fluids for chemical processing. *AIChE J.* **2001**, *47* (11), 2384–2389.

(13) Paulechka, Y. U.; Kabo, G. J.; Blokhin, A. V.; Vydrov, O. A.; Magee, J. W.; Frenkel, M. Thermodynamic properties of 1-butyl-3-methylimidazolium hexafluorophosphate in the ideal gas state. *J. Chem. Eng. Data* **2003**, *48* (3), 457–462.

(14) Domanska, U.; Bogel-Lukasik, R. Physicochemical properties and solubility of alkyl-(2-hydroxyethyl)-dimethylammonium bromide. *J. Phys. Chem. B* **2005**, *109* (24), 12124–12132.

(15) Welton, T. Room-temperature ionic liquids. Solvents for synthesis and catalysis. *Chem. Rev.* **1999**, *99* (8), 2071–2083.

(16) Rogers, R. D.; Seddon, K. R. Ionic liquids - Solvents of the future?. *Science* **2003**, *302* (5646), 792–793.

(17) Raeissi, S.; Peters, C. J. A potential ionic liquid for CO_2-separating gas membranes: selection and gas solubility studies. *Green Chem.* **2009**, *11* (2), 185–192.

(18) Muldoon, M. J.; Aki, S.; Anderson, J. L.; Dixon, J. K.; Brennecke, J. F. Improving carbon dioxide solubility in ionic liquids. *J. Phys. Chem. B* **2007**, *111* (30), 9001–9009.

(19) Anderson, J. L.; Dixon, J. K.; Brennecke, J. F. Solubility of CO_2, CH_4, C_2H_6, C_2H_4, O_2, and N_2 in 1-hexyl-3-methylpyridinium bis-(trifluoromethylsulfonyl)imide: Comparison to other ionic liquids. *Acc. Chem. Res.* **2007**, *40* (11), 1208–1216.

(20) Anthony, J. L.; Anderson, J. L.; Maginn, E. J.; Brennecke, J. F. Anion effects on gas solubility in ionic liquids. *J. Phys. Chem. B* **2005**, *109* (13), 6366–6374.

(21) Beckman, E. J. A challenge for green chemistry: designing molecules that readily dissolve in carbon dioxide. *Chem. Commun.* **2004**, *17*, 1885–1888.

(22) Jiang, Y. Y.; Wang, G. N.; Zhou, Z.; Wu, Y. T.; Geng, J.; Zhang, Z. B. Tetraalkylammonium amino acids as functionalized ionic liquids of low viscosity. *Chem. Commun.* **2008**, *4*, 505–507.

(23) Quinn, R.; Appleby, J. B.; Pez, G. P. Salt Hydrates - New Reversible Absorbents for Carbon-Dioxide. *J. Am. Chem. Soc.* **1995**, *117* (1), 329–335.

(24) Barrosse-Antle, L. E.; Compton, R. G. Reduction of carbon dioxide in 1-butyl-3-methylimidazolium acetate. *Chem. Commun.* **2009**, *25*, 3744–3746.

(25) McHale, G.; Hardacre, C.; Ge, R.; Doy, N.; Allen, R. W. K.; MacInnes, J. M.; Bown, M. R.; Newton, M. I. Density-viscosity product of small-volume ionic liquid samples using quartz crystal impedance analysis. *Anal. Chem.* **2008**, *80* (15), 5806–5811.

(26) Zhang, Y. Q.; Zhang, S. J.; Lu, X. M.; Zhou, Q.; Fan, W.; Zhang, X. P. Dual Amino-Functionalised Phosphonium Ionic Liquids for CO_2 Capture. *Chem.—Eur. J.* **2009**, *15* (12), 3003–3011.

(27) Quinn, R. Room temperature molten carboxylate salt hydrates. *Synth. React. Inorg., Met.-Org. Chem.* **2001**, *31* (3), 359–369.

(28) Widegren, J. A.; Laesecke, A.; Magee, J. W. The effect of dissolved water on the viscosities of hydrophobic room-temperature ionic liquids. *Chem. Commun.* **2005**, No. 12, 1610–1612.

(29) Shiflett, M. B.; Yokozeki, A. Phase Behavior of Carbon Dioxide in Ionic Liquids: [emim][Acetate], [emim][Trifluoroacetate], and [emim][Acetate] plus [emim][Trifluoroacetate] Mixtures. *J. Chem. Eng. Data* **2009**, *54* (1), 108–114.

(30) Cai, Q. H.; Hou, Y. W.; Shi, S. Y.; Lu, B.; Shan, Y. K. A novel ionic liquid based on small size cation. *Chin. Chem. Lett.* **2009**, *20* (1), 62–65.

(31) Matsumoto, H.; Kageyama, H.; Miyazaki, Y. Room temperature ionic liquids based on small aliphatic ammonium cations and asymmetric amide anions. *Chem. Commun.* **2002**, No. 16, 1726–1727.

(32) Seddon, K. R.; Stark, A.; Torres, M. J. In Influence of chloride, water, and organic solvents on the physical properties of ionic liquids. *15th International Conference on Physical Organic Chemistry (ICPOC 15)*, Gothenburg, Sweden, Jul 08–13, 2000; pp 2275–2287.

(33) Prausnitz, J. M.; Lichtenthaler, R. N.; Gomes de Azevedo, E. *Molecular Thermodynamics of Fluid-Phase Equilibria*, 3rd ed.; Prentice Hall: New York, 1998.

(34) Yokozeki, A.; Shiflett, M. B.; Junk, C. P.; Grieco, L. M.; Foo, T. Physical and Chemical Absorptions of Carbon Dioxide in Room-Temperature Ionic Liquids. *J. Phys. Chem. B* **2008**, *112* (51), 16654–16663.

(35) Scovazzo, P.; Camper, D.; Kieft, J.; Poshusta, J.; Koval, C.; Noble, R. Regular solution theory and CO_2 gas solubility in room-temperature ionic liquids. *Ind. Eng. Chem. Res.* **2004**, *43* (21), 6855–6860.

(36) Kumelan, J.; Kamps, A. P. S.; Tuma, D.; Yokozeki, A.; Shiflett, M. B.; Maurer, G. Solubility of tetrafluoromethane in the ionic liquid hmirn Tf2N. *J. Phys. Chem. B* **2008**, *112* (10), 3040–3047.

(37) Kamps, A. P. S.; Tuma, D.; Xia, J. Z.; Maurer, G. Solubility of CO_2 in the ionic liquid [bmim][PF6]. *J. Chem. Eng. Data* **2003**, *48* (3), 746–749.

(38) Cadours, R.; Bouallou, C.; Gaunand, A.; Richon, D. Kinetics of CO2 desorption from highly concentrated and CO_2-loaded methyl-diethanolamine aqueous solutions in the range 312−383 K. *Ind. Eng. Chem. Res.* **1997**, *36* (12), 5384–5391.

(39) Pani, F.; Gaunand, A.; Cadours, R.; Bouallou, C.; Richon, D. Kinetics of absorption of CO_2 in concentrated aqueous methyldietha-nolamine solutions in the range 296 to 343 K. *J. Chem. Eng. Data* **1997**, *42* (2), 353–359.